

Testing the presence of a dormant black hole inside HR 6819

A. Romagnolo¹ A. Olejak¹ A. Hypki¹ G. Wiktorowicz K. Belczynski¹

Nicolaus Copernicus Astronomical Center, The Polish Academy of Sciences, ul. Bartycka 18, 00-716 Warsaw, Poland
e-mail: aromagnolo@camk.edu.pl
chrisbelczynski@gmail.com

Received September 15, 1996; accepted March 16, 1997

ABSTRACT

Context. HR 6819 was reported in Rivinius et al. (2020) to be a triple system with a non-accreting black hole (BH). The inner binary system was defined as a B3 III type star with an estimated mass in the range $5 - 7 M_{\odot}$ and a dormant BH with a minimum mass of $4.2 M_{\odot}$. The period of the inner binary was estimated to be ~ 40 days with an eccentricity in the range $0.02 - 0.04$. As the inner binary is not resolved, the third component may actually be just spatially coinciding with the inner binary.

Aims. In our study we check if the system's inner binary can be reconstructed using the isolated binary formation channel in the Galactic field or the dynamical one within globular star clusters. Our goals are to understand the formation of the inner binary and to test the presence of a non-accreting BH as the unseen companion of the B3 III type star.

Methods. To simulate the inner binary evolution we assumed that the influence of the third body on the formation of the inner binary is negligible. We tested various models with different values of physical parameters such as the mass loss rate during BH formation or the efficiency of orbital energy loss for common envelope ejection.

Results. We found that the reported masses and orbital parameters of the HR 6819 inner binary can be reconstructed using isolated binary evolution. By comparing the Roche lobe radii with the respective stellar radii no mass transfer event was shown to happen for more than 40 Myr after the BH collapse, suggesting that no accretion disk is supposed to form around the BH during the BH-MS phase. Our evolutionary scenarios are therefore compatible with the existence of a dormant black hole in this system. We can reconstruct the system with isolated binaries, although in our simulations we had to use non-standard parameter values and to assume no asymmetric mass ejection during the black hole collapse. Out of the whole synthetic Galactic disk BH population only 0.0001% of the BH-MS binaries fall within the observational constraints. According to our simulations, we expect only few binaries in the Galactic globular clusters to be potential candidates for the HR 6819 system. However, all of them have significantly larger eccentricities (> 0.3) than the desired one.

Conclusions. Our statistical analysis suggests that despite the HR 6819 inner binary can be reconstructed with isolated binary evolution, this evolutionary channel is unlikely to reproduce its reported parameters. Under the initial assumption that the outer star doesn't impact the evolution of its inner binary, we argue that the absence of a third body proposed by El-Badry & Quataert (2021) and Bodensteiner, J. et al. (2020) might be a more natural explanation for the given observational data.

Key words. Binaries - Stars: black holes - Stars: individual: HR 6819

1. Introduction

Black holes (BH) in binary systems are predicted to be around 10% of the whole Milky Way BH population, and most of them are BH-BH systems (Olejak et al. 2020a). BHs with non-compact companions can be detected through interactions with them, but they are possibly a very small fraction of the total Galactic population. So far only ~ 20 Galactic BH systems have been detected (Casares 2007; Casares & Jonker 2014)¹. Most of them are close X-ray binary systems transferring matter through an accretion disk. For recent reviews on stellar-origin BHs see Bambi (2018). BHs may also be detected as gravitational wave signal emitters (Abbott et al. 2016) and in non-interacting binaries using astrometric and spectroscopic observations of their companion stars. Single BHs can also be potentially detected through microlensing (e.g. Wyrzykowski et al. 2016) or while accreting from interstellar medium (Tsuna et al. 2018). Theoretically Hawking radiation (Hawking 1974) may possibly allow for a detection of thermal radiation from the immediate

vicinity of a BH.

HR 6819 is reported to be a triple system harbouring a BH candidate (Rivinius et al. 2020). The BH candidate mass was estimated on the basis of radial motions of the visible star in the inner binary. The spectral type of the companion star has been classified as B3 III. Using single-star evolutionary tracks (Ekström et al. 2012) and observational data (Hohle et al. 2010), the most likely range for the star was estimated to be between 5 and $7 M_{\odot}$, while the lower limit for the BH candidate mass was set at $4.2 M_{\odot}$. The star was reported to be roughly $1 M_{\odot}$ more massive than its unseen companion, while the inner binary is supposed to have a period of 40.333 ± 0.004 and an eccentricity of 0.03 ± 0.01 . The outer orbit with the Be star (with a mass of $\sim 6 M_{\odot}$) is instead unconstrained. On top of that, the outer star does not show any significant radial velocity variation and may actually be just spatially coinciding with the inner binary. Neither the FEROS spectrometer (Rivinius et al. 2020), nor *Gaia* have a sufficient resolution to resolve the full triple system. The age of the whole triple system was estimated to be between 15 and 75 Myr. Other possible interpretations of the observational data cannot be nevertheless excluded. For

¹ <https://stellarcollapse.org/sites/default/files/table.pdf>

instance, the absence of a combined Balmer line depth $\sim 6\%$ in the spectra from Rivinius et al. (2020) suggests that the unseen companion of the inner binary might not be a dormant black hole, but rather a close binary in a 4-day period, composed of two A0 stars of $\sim 2.3 M_{\odot}$ each (Mazeh & Faigler 2020). In an independent analysis of the system spectrum El-Badry & Quataert (2021) also proposed the absence of a dormant BH. In this way HR 6819 would only be composed by its visible components, i.e. the B3 star and its Be stellar companion. Also Bodensteiner, J. et al. (2020) proposed a similar solution. According to their study HR 6819 could be a binary composed by a stripped B-type star and a rapidly-rotating Be companion. Post-interaction lower-mass stars (exposed hot cores) can also mimic higher-mass stars evolving in isolation or in non-interacting binaries. The temperature of B-type subdwarfs can be higher than 20 kK despite having masses $\lesssim 1 M_{\odot}$ (e.g. Heber 2009).

In our study we assume that HR 6819 is a triple system with either the third component unbound to the inner binary or the outer orbit so wide that it does not affect its evolution. We consequently adopted the estimates from Rivinius et al. (2020) as reference parameters for HR 6819-like systems. We used the isolated binary evolution scenario in the Galactic field as well as the dynamical formation scenario in globular clusters.

2. Method

2.1. StarTrack

In our study we used the StarTrack² population synthesis code (Belczynski et al. 2002, 2008), which allows the user to simulate the isolated binary evolution of the system with a wide variety of initial conditions and physical parameters. The most up to date description of StarTrack’s standard physical parameters and approaches, as well as the adopted model for star formation rates and the metallicity distribution of the Universe, can be found in Belczynski et al. (2020), with two updates in §2 of Olejak et al. (2020b). We used a delayed SN engine model that allows the formation of NS/BH within the lower mass gap: $2 - 5 M_{\odot}$ (Belczynski et al. 2012; Fryer et al. 2012).

We introduced a significant modification compared to the StarTrack standard assumptions, which is that all BHs (regardless of their mass) are formed via direct collapse without asymmetric mass ejection in SN explosions. In such scenario, BHs do not receive natal kicks except for potential Blaauw kicks (Blaauw 1961).

In our simulations we tested several scenarios with different values of metallicity Z (see Table 1), neutrino mass loss during BH collapse F_{loss} (in terms of percentage of total mass loss), efficiency of orbital energy loss for CE ejections α , the initial system semi-major axis a_0 , and the stellar masses of progenitors at ZAMS, respectively $M_{\text{ZAMS,a}}$ and $M_{\text{ZAMS,b}}$.

Table 1: Tested parameter space for the isolated binary evolution of HR 6819. Here Z -metallicity, F_{loss} -neutrino mass loss during BH formation, α -efficiency of orbital energy loss for CE ejection, $M_{\text{ZAMS,a/b}}$ - masses at ZAMS of respectively the BH progenitor star and its stellar companion, and a_0 - initial semi-major axis.

Parameter	Min	Max
Z	0.01	0.014
F_{loss}	1%	20%
α	0.5	5
$M_{\text{ZAMS,a}} [M_{\odot}]$	10	150
$M_{\text{ZAMS,b}} [M_{\odot}]$	0.08	150
$a_0 [R_{\odot}]$	2000	10000

2.2. MOCCA

To investigate a possible dynamical interactions influence on the formation of HR 6819 within globular star clusters we used already existing numerical models of so-called MOCCA-SURVEY-2 which were computed with the MOCCA code³. This is currently one of the most advanced codes to perform full stellar and dynamical evolution of real size star clusters (Giersz et al. 2014; Hypki & Giersz 2013; Giersz 1998). MOCCA is already used in a wide number of projects to investigate the evolution of compact binaries e.g. BHs binaries (Hong et al. 2020). Moreover, it is able to follow N-body codes very precisely and it provides almost as much information about stars and binary stars (Wang et al. 2016). The stellar evolution in MOCCA is performed with the SSE/BSE code (Hurley et al. 2000, 2002), while the strong dynamical interactions with the Fewbody code (Fregeau et al. 2004). The newest version of MOCCA was recently used to perform another MOCCA-SURVEY-2 – a large number of numerical simulations with various initial conditions to mimic the properties of the globular clusters observed in our Galaxy. The most important new feature of MOCCA is the ability to follow the dynamical evolution of multiple stellar populations. Multiple populations are different populations of stars identified from the color spread in the color-magnitude diagram of a GC or the chromosome diagram. They were observed in almost all GCs (Piotto et al. 2015) and that challenges the traditional understanding that all stars in a GC were born in the same environment and with the same chemical composition. The new set of simulations was performed to study in detail the dynamical mixing between these populations, but it is equally good at performing research on compact objects. MOCCA-SURVEY-2 currently contains over 250 very detailed models which cover broad ranges of initial conditions (see Table 2). Among the many initial parameters for MOCCA the one which might have an outstanding importance for this research is the flag that determines the mass for NS and BH formation. For MOCCA-SURVEY-2 the rapid and the delayed supernova models from Fryer et al. (2012) were applied in order to have some BH population within the first mass gap range ($2 - 5 M_{\odot}$). The metallicity for all models is 0.001 (1/200 of the solar metallicity). Models with various metallicities are planned for the next stage of the MOCCA-SURVEY-2. Wind prescriptions were chosen to be similar to Belczynski et al. (2010). Kick mechanism for BH and NS formation are the same and for MOCCA-SURVEY-2 we used standard momentum-conserving kick velocity distribution (265 km/s, Maxwellian). Moreover, kicks work for both single, and binary stars. Pulsational pair instability (PPISN) and full-fledged pair-instability supernova (PISN) were chosen to follow

² <https://startrackworks.camk.edu.pl>

³ <http://moccacode.net>

Belczynski et al. (2016). Possibility for the electron capture SNs is switched on. Kick velocity is modified because of mass fallback on BH according to Belczynski et al. (2002); Belczynski et al. (2006).

Table 2: Summary of initial conditions for MOCCA used to perform MOCCA-SURVEY-2 simulations: **n1**, **n2** – number of single stars and binaries for population 1 and 2 respectively; **fracb1**, **fracb2** – initial binary fraction for populations 1 and 2 (using n1, and n2 values one can compute the number of single and binary stars for every population); **w01**, **w02** – King model parameters for population 1 and 2; **mup1**, **mup2** – upper mass limit for a new star for population 1 and 2 (M_{\odot}), lower limit is 0.08 M_{\odot} ; **rbar** – tidal radius for the whole star cluster (pc); **rh_mcl** – half mass radius for the whole star cluster (pc); **conc_pop** – concentration parameter between different populations defined as the ratio between half-mass radius of the population 2 over the half mass radius of the population 1 (R_{h2}/R_{h1}). If a parameter contains multiple values it means that there was performed a combination between multiple parameters in order to create one instance of initial conditions for one mocca simulation (n1 = 400k with n2 = 200k, n1 = 400k with n2 = 400k, n1 = 400k with n2 = 600k etc.).

Parameter	Values
n1	400k
n2	200k, 400k, 600k
fracb1,fracb2	0.1, 0.95
w01	6
w02	6, 8
mup1	150
mup2	50, 150
rbar	60, 120
rh_mcl	0.6, 1.2, 2, 4, 6
conc_pop	0.1, 0.2, 0.5, 1, 1.5

3. Isolated binary evolution

In order to reconstruct the HR 6819 inner binary we had to retrieve some scenarios that, similarly to Rivinius et al. (2020), gave a BH-MS binary whose stellar masses are $> 4.2 M_{\odot}$ for the BH and between 5 and 7 M_{\odot} for the visible companion. Additionally the two objects are supposed to roughly differ of 1 M_{\odot} . Finally, the observational constraints require an orbital period of 40.3 days and an eccentricity around 0.03.

From now on we will refer to the BH progenitor as the primary star and its stellar companion as the secondary star.

3.1. Example of an evolutionary scenario

Here we present an example of the optimal evolutionary scenarios (Fig. 1) that leads to the formation of a binary that matches the observational constraints from Rivinius et al. (2020). Initially the system consists at ZAMS of two stars of 24.0 M_{\odot} and 7 M_{\odot} at a metallicity Z of 0.0105. For the given example, the adopted value for neutrino mass loss F_{loss} is 7%, while the CE ejection efficiency parameter α is 5.

At the beginning the two stars are on a very wide, circular orbit (period $\sim 2.6 \times 10^3$ days, $e = 0.0$). For more than 8 Myr the secondary star remains unaltered in its main sequence (MS), while the primary star expands and evolves into a core helium burning giant. The system then evolves thorough a common envelope (CE) phase, after which the orbital period is reduced to

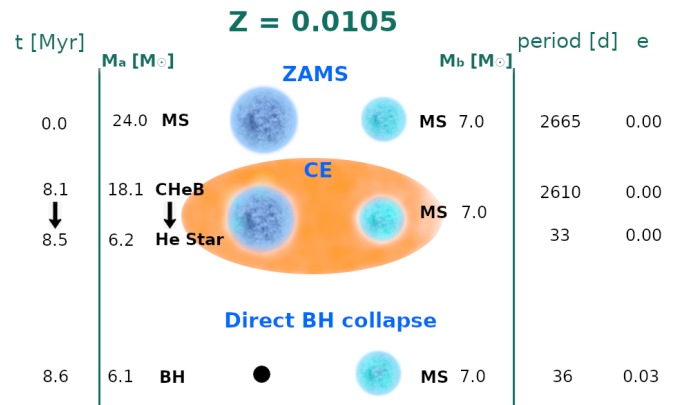


Fig. 1: Formation of a system resembling the HR 6819 inner binary. It starts from two massive stars at metallicity $Z = 0.0105$. While the companion star remains in its main sequence, the more massive star initiates a CE phase after ~ 8.5 Myr and shortly after it collapses into a BH.

about 30 days and the giant star loses its envelope. We then assume a direct collapse of the primary star into a BH. Due to the neutrinos emission, the eccentricity of the system slightly increases to $e = 0.03$.

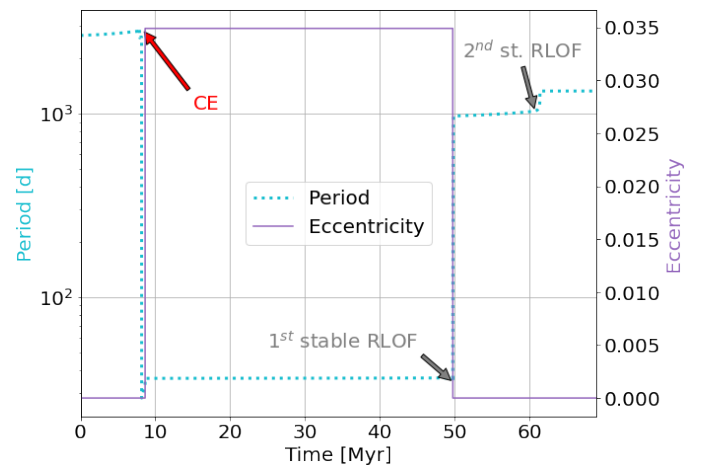


Fig. 2: Evolution of the binary period (in light blue) and eccentricity (in purple). The CE phase (in red) took place around 8.2 Myr and was initiated by the primary star, while the first and the second stable RLOF phases (in grey) happened respectively around 49 Myr and 61 Myr, and were initiated by the secondary star.

The orbital period during the whole BH-MS phase (roughly between 10 and 50 Myr since the system formation), as shown in Fig. 2 is ~ 36 d, which is consistent with the reported value 40.3 d. The eccentricity is also in the estimated [0.02; 0.04] range.

The B3 III star, as shown in Fig. 3, during the first 50 Myr has a mass of 7 M_{\odot} , which is the observational upper limit from Rivinius et al. (2020). The reconstructed BH mass 6.1 M_{\odot} is above the minimum observational limit of 4.2 M_{\odot} and fulfills the requirement derived from mass function calculations. During the BH-MS phase the difference in mass between the BH and its stellar companion in the inner binary is consistent with the estimated value $\Delta M = 1 M_{\odot}$.

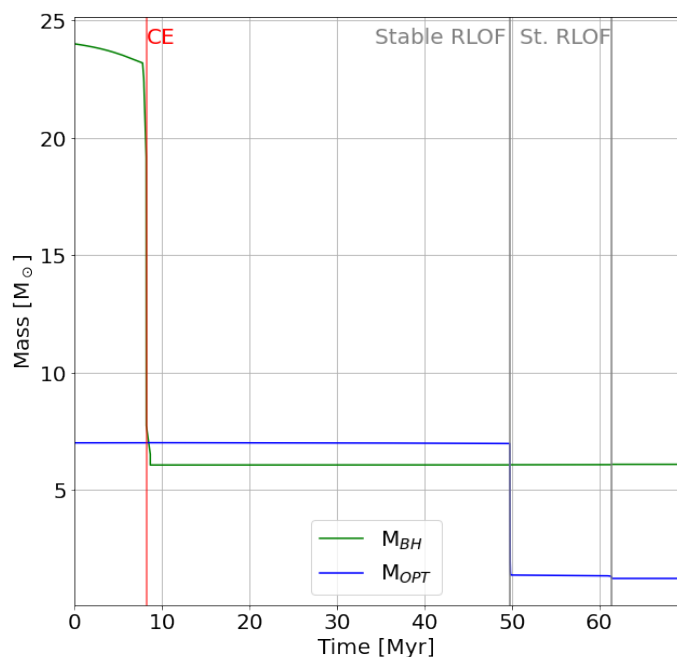


Fig. 3: Temporal mass evolution of the two stars in the inner binary. The black-hole progenitor (green line) loses most of its mass during the CE phase (red line) and collapses into a BH within 8.64 Myr. The B3 III star (blue line), instead, remains its MS phase until it transforms into a Hertzsprung gap star and initiates its first Roche Lobe phase (grey line) at around 50 Myr, when it loses $\sim 80\%$ of its mass and evolves into a He MS star.

In Fig. 4 we show the temporal evolution of the radii of the two stars in the tested binary (BH above and the secondary star below) in comparison with their Roche lobe radii. We note that during BH-MS stage (time between 8.64 and 49.77 Myr) there is no RLOF episode and the wind mass loss from the secondary star ($\dot{M} < 10^{-7} M_{\odot} \text{ yr}^{-1}$) is too weak to produce any significant X-ray emission at the orbital separation found for this system ($a \sim 108 R_{\odot}$) during this stage. The BH in our example is thus dormant and in agreement with the observational data.

3.2. Optimal parameter space

We tested the initial parameter values within the ranges given in Table 1. We found that the HR 6819 inner binary can be reconstructed with isolated binary evolution within a narrow parameter space. Our best fits require a primary star between 18 and 26 M_{\odot} and a secondary star between 5 and 7 M_{\odot} at ZAMS. In order to reconstruct the lower limit on the BH mass and the estimated mass difference between the two stellar objects of the order of 1 M_{\odot} , we needed to choose an initial metallicity and a semi-major axis respectively in the ranges [0.01; 0.02] and [2600; 2630] R_{\odot} , although partial matches (i.e. at least two parameters matching the observational constraints) also arise with a wider set of initial orbital separations (between 2300 and 2800 R_{\odot}). The optimal neutrino mass loss factor F_{loss} needed to obtain both a post-collapse eccentricity e in the range [0.02; 0.04] and an estimated orbital period ~ 40 days was found to be a fraction between 5-8% of the pre-collapse mass. In our calculations we needed to use high, non-standard values for the efficiency of the CE orbital energy loss ($\alpha > 4.5 M_{\odot}$). This is far from our standard adopted value of $\alpha = 1$, although simulations including

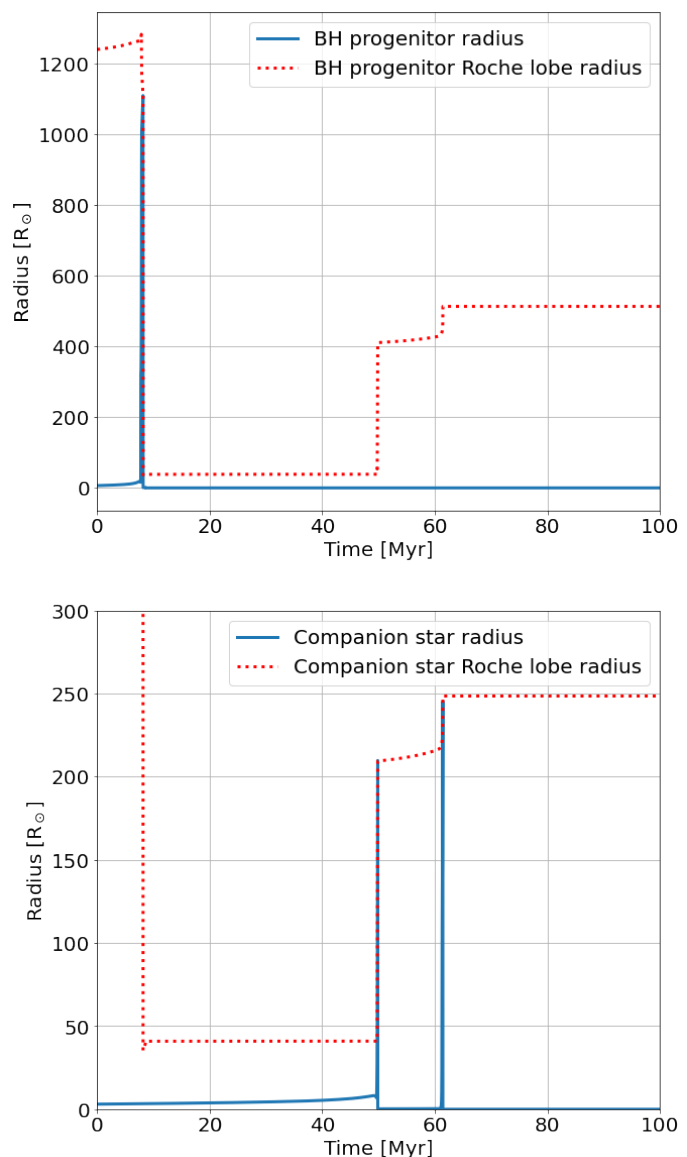


Fig. 4: Comparison between the temporal evolution of the BH (above) and the visible companion (below) radii (in blue) and their respective Roche lobe radii (dotted red). After the BH collapse neither of the stars go beyond their Roche lobe until ~ 50 Myr, when the companion star will leave its main sequence, expand and initiate the mass transfer.

more physical processes such as accretion show that the effective α can be as high as 5 (Fragos et al. 2019). These results have been already adopted in some population synthesis studies (e.g. Santoliquido et al. 2020). The use of lower values of α in our simulations causes a drastic decrease of the post-CE orbital period for the reconstructed systems. In Table 3 the final ranges for the reconstructed masses of the two components, their mass difference and the orbital period and eccentricity that we retrieved for the post-BH collapse phase are shown. These results are then compared to the observational results from Rivinius et al. (2020), which are also shown on the rightmost column.

Additionally, we compared the radial evolution of the BH progenitor from StarTrack (and therefore the start of mass transfer events), with the one of a star with the same ZAMS mass and metallicity simulated with Modules for Experiments in Stel-

Table 3: Comparison between the minimum and maximum reconstructed inner binary parameters and the observational constraints from Rivinius et al. (2020). Here we list: the BH formation mass M_{BH} , the mass of the B3 III star M_{OPT} during the BH-MS phase, the mass difference ΔM between the two companions, the orbital period and the orbital eccentricity e .

Parameter	Min	Max	Rivinius et al. (2020)
M_{BH} [M_{\odot}]	5.6	6.4	> 4.2
M_{OPT} [M_{\odot}]	6.8	7	[5;7]
ΔM	0.6	1.4	1
Period [d]	30	50	40.333 ± 0.004
e	0.004	0.05	0.03 ± 0.01

lar Astrophysics (MESA) (Paxton et al. 2011, 2013, 2015, 2018, 2019). In this chosen parameter space the temporal difference between the start of a CE phase with MESA and STARTRACK is usually in the order of $\sim 2\%$, showing therefore a good agreement between the two codes for this specific case. For more details see Appendix A.

3.3. Future evolution of the inner binary

In Figures 2, 3, and 4 we present our forecast for the future evolution of the considered binary system parameters, i.e. stellar masses, radii and orbital parameters. During the whole BH-MS phase these parameters remain almost unchanged with the only exception of the radius of the secondary star, which increases from $\sim 3 R_{\odot}$ to roughly $6 R_{\odot}$ as it evolves through its main sequence. According to our STARTRACK evolutionary tracks, at the age of ~ 50 Myr, after evolving off its MS phase, the secondary star begins a rapid expansion and it will eventually fill its Roche lobe. The system will then enter stable mass transfer phase which will last for approximately 0.1 Myr. After that the released orbital energy provides the kinetic energy needed for the outward ejection of the envelope and the star will evolve into a naked He star of $\sim 1.37 M_{\odot}$. Due to this orbital energy loss the binary period will significantly expand to $\sim 10^3$ d ($a \sim 104.75$ AU), while the orbit itself will get circularized. The secondary star will then pass into its giant phase and later initiate its second RLOF at ~ 61 Myr. The orbital period will then increase to roughly 1279 days (~ 962 AU) and after that the secondary star will have lost more than 80% of its mass since ZAMS. It will then finally evolve into a carbon-oxygen white dwarf (WD).

The final values for the binary are described in Table 4:

Table 4: Final values for the simulated BH-WD binary.

Parameter	ZAMS	Final
M_{BH} [M_{\odot}]	24	6.08
M_{OPT} [M_{\odot}]	7	1.23
Period [d]	2665.16	1279.73
e	0.00	0.00

3.4. Statistical significance

To estimate the likelihood of a BH-MS system that resembles the HR 6819 inner binary to form in the thin disk of the Milky Way, we used a stellar formation rate (SFR) of $\sim 5 M_{\odot} \text{ yr}^{-1}$, similarly to Olejak et al. (2020a). We assumed the SFR to be constant over the whole simulated 10 Gyr. We then post-processed our

population of 10M binaries by iterating each system from different starting points in time. With this method we were able to generate a whole Galactic disk population where each system is realistically born at different times and doesn't simply start its existence at $t=0$ with all the others. This consequently means that, at our time, many binaries are either too young for their most massive star to collapse into a BH or too old for the optical companion to exist in its MS phase. The ratio between the sum of all the simulated single and binary stars' ZAMS masses M_{sum} and the Galactic disk stellar mass M_{gal} gives us the scale factor f_{scale} to be finally used to retrieve the final number of BH-MS binaries that currently exist in our Galactic disk.

$$f_{scale} = \frac{M_{gal}}{M_{sum}} \quad (1)$$

In our case $M_{gal} = 5 \times 10^{10}$ and $M_{sum} \sim 10.3 \times 10^7$, which lead to a f_{scale} of roughly 0.0021.

$$n_{final}^* = n_{sim}^* \times f_{scale} \quad (2)$$

With n_{sim}^* the number of binaries from our combined StarTrack and post-processing simulations, and n_{final}^* the Galactic number estimate for BH-MS binaries. The final number of BHs in binary systems that we retrieved in this way is $\sim 8.3 \times 10^6$, which is in agreement with the synthetic BH catalogue from Olejak et al. (2020a).

We then computed the *total difference*, which in this case is a number measuring how a given binary differs from HR 6819, by taking into account the desired set of parameters (BH mass $\sim 4.2 - 6 M_{\odot}$, main-sequence companion $\sim 5 - 7 M_{\odot}$, period ~ 40 days⁴, eccentricity 0.02 – 0.04). If its total difference is equal to 1.0 it means that a binary has the parameters within the requested ranges, if the value is larger than 1.0 it means that some of the parameters are getting outside the observational constraints. The difference for any of the four parameters (BH mass, companion mass, period and eccentricity) is measured as a normalized difference to the middle of the expected center of a range. These normalized differences for the the secondary star mass, the BH mass, the binary period and the eccentricity are then respectively calculated in the following way:

$$Comp_{diff}(x) = \begin{cases} ABS(M_{comp} - 5.0)/6.0 + 1.0, & \text{if } M_{comp} < 5 \\ ABS(M_{comp} - 7.0)/6.0 + 1.0, & \text{if } M_{comp} > 7 \\ 1.0, & \text{otherwise} \end{cases} \quad (3)$$

$$BH_{diff}(x) = \begin{cases} ABS(M_{BH} - 4.2)/5.1 + 1.0, & \text{if } M_{BH} < 4.2 \\ ABS(M_{BH} - 6.0)/5.1 + 1.0, & \text{if } M_{BH} > 6 \\ 1.0, & \text{otherwise} \end{cases} \quad (4)$$

$$Per_{diff}(x) = \begin{cases} ABS(M_{Per} - 30)/40 + 1.0, & \text{if } M_{Per} < 30 \\ ABS(M_{Per} - 50)/40 + 1.0, & \text{if } M_{Per} > 50 \\ 1.0, & \text{otherwise} \end{cases} \quad (5)$$

⁴ We set an arbitrary confidence range of 10 days around this value, which doesn't correspond to the actual margin of error (0.004 days) reported in Rivinius et al. (2020).

$$Ecc_{\text{diff}}(x) = \begin{cases} ABS(M_{\text{Ecc}} - 0.02)/0.03 + 1.0, & \text{if } M_{\text{Ecc}} < 0.02 \\ ABS(M_{\text{Ecc}} - 0.04)/0.03 + 1.0, & \text{if } M_{\text{Ecc}} > 0.04 \\ 1.0, & \text{otherwise} \end{cases} \quad (6)$$

The final total difference (presented on Fig. 5 and Fig. 6), is a combination of the four differences:

$$Total_{\text{diff}} = BH_{\text{diff}} \times Comp_{\text{diff}} \times Per_{\text{diff}} \times Ecc_{\text{diff}} \quad (7)$$

If all the four parameters are within the set ranges and there is therefore a complete agreement with our predictions, the total difference will be equal to 1. As a reference, with $Total_{\text{diff}} = 2$, a binary could have the secondary star mass equal to $8.13 M_{\odot}$, a BH mass of $6.96 M_{\odot}$, an orbital period of 57.57 days, and an eccentricity of 0.0456.

The amount of optimal HR 6819 candidates that fall within a total difference of 1 is almost null. More precisely only the 0.0001% (corresponding to 82 BH-MS binaries) of our synthetic BH-MS binaries in the Galactic disk have a total difference of 1 and can be considered as good candidates for the HR 6819 inner binary. This result suggests that a system like the one described in Rivinius et al. (2020) for HR 6819, despite being compatible with our evolutionary scenarios, is extremely unlikely to form and consequently to be detected.

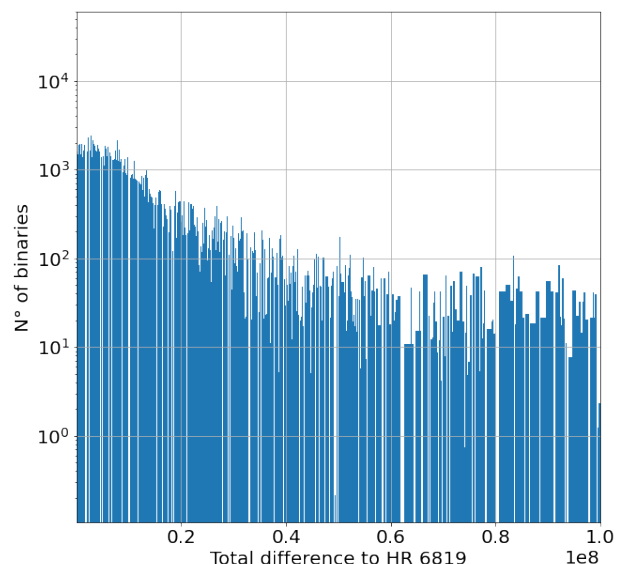
4. Possible dynamical origin of HR 6819 within star clusters

The MOCCA-SURVEY-2 simulations were used to find possible matches for the HR 6819 inner binary. Every MOCCA simulation consists of around 20 files. Among others there are files which store information about every stellar evolution event (e.g. mass transfer, mass loss, typically dozens of millions of events) and dynamical interactions (typically a few millions) for all stars in the star cluster. This allows to build the full history of stellar formation and evolution, and also the entire dynamical history for every star. The search for possible HR 6819 candidates was conducted among all simulations and within every output file. The search for a possible match was performed on already computed simulations.

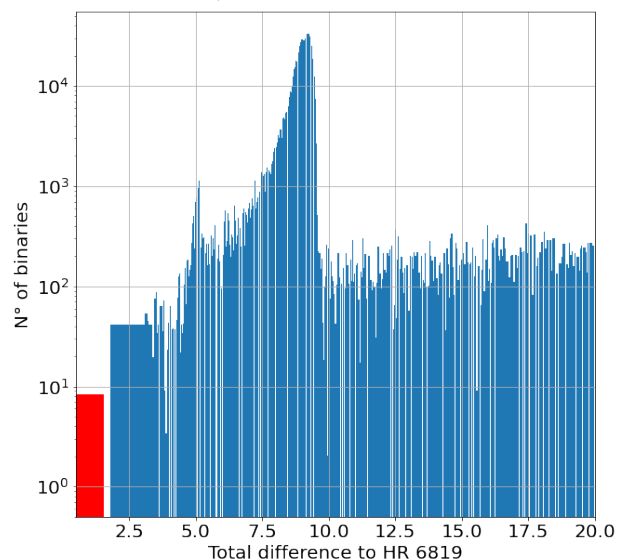
As a result of applying filters for the BH mass ($\sim 4 - 6 M_{\odot}$), the secondary star mass ($\sim 5 - 7 M_{\odot}$) during MS, and the orbital period and eccentricity of any value, only one binary system was found to match the observational constraints with rapid supernova models and only three with delayed supernova models (Fryer et al. 2012).

For rapid SN models there is a mass gap where BHs do not form. However, it is interesting to see that even for the initially very dense MOCCA models for which dynamical mergers are frequent, the number of BHs falling into that range does not increase. The potential candidate that was found (BH mass = $5.2 M_{\odot}$, secondary star MS mass = $6.6 M_{\odot}$, semi-major axis = $155 R_{\odot}$, eccentricity = 0.69) has a period over 50 days and an eccentricity which is much larger than expected. Before having this set of parameters the binary had seven binary-binary and binary-single dynamical interactions in which semi-major axes and eccentricities were changed only by a few percent. As a conclusion this binary hardly matches the HR 6819 system.

For the delayed SN models we observed many BH masses within the BH mass gap, but the required parameters for their



(a) Total difference over the whole population of BH-MS binaries. The X-axis values are scaled by 10^8 .



(b) BH-MS binaries with a total difference smaller than 20. The red column represents the amount of BH-MS binaries with a total difference of 1.

Fig. 5: Histograms representing the number of BH-MS binaries (vertical axis) for each total differences (horizontal axis) between their masses, orbital period and eccentricity, and the ranges provided by the HR 6819 observational constraints from Rivinius et al. (2020).

companions ruled them out. The only exceptions were three binaries whose masses fall in the desired range, but only for one of them the period matches the set constraints ($T = 27 \text{ Myr}$, BH mass = $5.69 M_{\odot}$, secondary star MS mass = $6.06 M_{\odot}$, semi-major axis = $111 R_{\odot}$, period = 41.96 days, eccentricity = 0.3). However, in this case the eccentricity 0.3 is also significantly larger than the expected one (0.02 – 0.04). This is the closest possible match to HR 6819 found in MOCCA-SURVEY-2 simulations.

4.1. Statistical significance of the results for possible dynamical formation

Among all *MOCCA* simulations only four reliable candidates for the system HR 6819 were found. Only one of them, ignoring strict requirements for eccentricity, may be considered as a candidate. It is important to check how statistically significant this result is and to make sure that finding only one or two candidates is not only due to a selection bias. In available *MOCCA-SURVEY-2* simulations we have found the histories of all BH binaries (all stellar and dynamical events that happened for any binary which at some point was consisting of a BH and any companion).

Like in section 3.4, we calculated the total difference between the simulated BH-MS binaries and the HR 6819 observational constraints. The procedure to estimate how statistically significant are HR 6819 candidates from *MOCCA-SURVEY-2* simulations is very simple and it was done in the following way. We computed the total mass of the Milky Way GCs by taking the masses estimates from Baumgardt (2017)⁵ and got the total GCs mass equal to $3.7 \times 10^7 M_{\odot}$. Mass loss of the star clusters through the Hubble time depends on many factors (e.g. Meiron et al. (2021)). For the sake of simplicity we took the assumption that half of the mass of a star cluster could be lost for a typical GC. Thus, we assume the initial mass for Milky Way GCs to be $7.4 \times 10^7 M_{\odot}$. As a last step we selected one typical GC model from *MOCCA-SURVEY-2* with initial 800k stars, 95% initial binaries, tidal radius of 60 pc and initial half-mass radius of 1.2 pc (the size, and the density of this model fits to the middle of possible values from *MOCCA-SURVEY-2*). We multiplied the number of binary candidates from this simulation to match the total initial mass of all Milky Way GCs. The resulting histogram with $Total_{diff}$ values for all BH binaries, candidates for the system HR 6819, is presented in Fig. 6. The Figure shows that there is only a very few candidates with similar properties to the HR 6819 inner binary (on the very left side of the histogram). On the bottom plot in Fig. 6 there is a close-up of the histogram up to values of 60.0. The plots show that it is really hard to find candidates for HR 6819 with *MOCCA* simulations – the vast majority of possible binaries differs around 20 times in terms of the values of the HR 6819 system. The long tail of values (> 60.0) in the histogram on the top panel in Fig. 6 is mainly caused by binaries with much larger periods than the desired 40 days (the period is many times larger than 40, thus the total difference gets very high as well).

The main reason why it is hard to find dynamical candidates for HR 6819 system among *MOCCA* simulation is due to the initial conditions, the stellar evolution code used in *MOCCA* simulations and the fact that possible candidates may be found only in the very beginning of the star clusters simulations. Initial conditions are crucial when it comes to a population of BHs in the system. In *MOCCA-SURVEY-2* simulations we use e.g. two rapid and delayed supernova models (Fryer et al. 2012) which have a great influence to the masses of newly created BHs. There are other initial conditions which might play a role here and based on the Section 3 one can say that a proper selection of initial conditions is crucial. When it comes to stellar evolution codes we have to stress out that the *MOCCA* simulations were done with *SSE/BSE* code Hurley et al. (2000, 2002) which differs in details to *STARTRACK* code.

However, the most important factor when it comes to a possible dynamical origin of HR 6819-like systems comes from how star clusters evolve in the first dozens (up to hundreds) of Myrs.

⁵ <https://people.smp.uq.edu.au/HolgerBaumgardt/globular/>

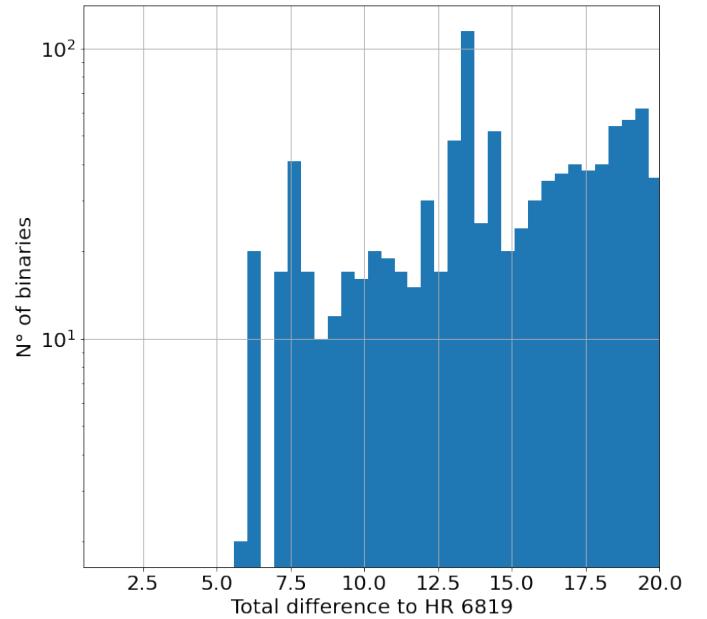


Fig. 6: The plot shows how likely is the formation of HR 6819 candidates in star clusters performed with the *MOCCA* numerical simulations. The values on the X axis are the total differences to HR 6819. 1.0 means that it is a strong candidate with parameters well within the expected ones, and all the values larger than 1.0 are a measure of how many times a binary exceeds the desired parameters (for details see Section 3.4). The Y values identify the number of binaries for a given bin.

The first stage of GCs evolution is mainly caused by the stellar evolution, not by the dynamics. The star clusters, due to the presence of massive stars, lose a lot of mass during the initial stages of star clusters evolution. Due to mass loss the star clusters can expand significantly and this in turn slows any dynamical process that might happen between stars. Some strong dynamical interactions could happen basically only in the very central regions of star clusters. Only after several hundreds of Myrs the core starts to contract and the influence of some strong dynamical interactions can have some non-negligible effects of the populations of some stars (e.g. compact BH binaries). Thus, dynamical origin for potential HR 6819 is very unlikely.

5. Conclusion

In our study we test if either the isolated or the dynamical evolution may be used in order to reconstruct the inner binary of the HR 8619 triple system and at the same time to verify the actual possibility that a dormant black-hole can be the unseen companion of the B3 star. To do so, we set our models in order to recreate the conditions described in Rivinius et al. (2020) with the following two assumptions:

- HR 6819 is a triple system
- The third, "outside" component of HR 8619 is either unbound or its effect on the inner binary formation is negligible

To obtain a good agreement with the observational constraints, the isolated binary channel requires the adoption of non-standard values for some physical parameters. We find that non-standard choices on several physical processes are needed to reproduce the HR inner binary in isolated binary evolution. In particular, we can match the observed properties of the HR 6819

system for high CE efficiency ($\alpha_{CE} = 5$), and if we allow for direct BH formation even for low-mass BHs. In the simulated scenarios the inner binary was initially a wide binary system with ZAMS stellar masses of 24 and 7 M_{\odot} , and a metallicity $Z \approx 0.01$. The high value of CE efficiency was required to decrease the orbital period of a binary to the observed value. This particular evolutionary part was the key in forming HR-like systems.

We also considered a dynamical formation scenario which could take place in globular clusters. Dynamical interactions in dense star cluster environments could play an important role in the formation of binary systems. We checked if such interactions increase the likelihood of reconstructing an HR 6819-like system. We investigated all models available within MOCCA-SURVEY-2 models and found only a few possible candidates. None of them had the expected eccentricity, though.

Considering the observational constraints and our evolutionary scenarios, our work shows that the presence of a dormant non-accreting black hole in the inner binary of HR 6819 is a plausible option. Nevertheless, despite the HR 6819 inner binary can be reproduced by isolated binary evolution, our statistical analysis suggests that it is highly unlikely to find one, given the very low formation efficiency. Considering these results, we suggest that other options to explain the HR 6819 inner binary should be considered. For instance, the absence of the third unseen body that was proposed by El-Badry & Quataert (2021) and Bodensteiner, J. et al. (2020) might be a more natural explanation for the given observational data.

Acknowledgements. AR, AO, AH, KB and acknowledge support from the Polish National Science Center (NCN) grant Maestro (2018/30/A/ST9/00050).

References

- Abbott, B. P., Abbott, R., Abbott, T. D., et al. 2016, *Physical Review X*, 6, 041015
- Bambi, C. 2018, *Annalen der Physik*, 530, 1700430
- Baumgardt, H. 2017, *MNRAS*, 464, 2174
- Belczynski, K., Bulik, T., Fryer, C. L., et al. 2010, *The Astrophysical Journal*, 714, 1217–1226
- Belczynski, K., Heger, A., Gladysz, W., et al. 2016, *A&A*, 594, A97
- Belczynski, K., Kalogera, V., & Bulik, T. 2002, *The Astrophysical Journal*, 572, 407
- Belczynski, K., Kalogera, V., Rasio, F. A., et al. 2008, *The Astrophysical Journal Supplement Series*, 174, 223
- Belczynski, K., Klencki, J., Fields, C. E., et al. 2020, *A&A*, 636, A104
- Belczynski, K., Sadowski, A., Rasio, F. A., & Bulik, T. 2006, *ApJ*, 650, 303
- Belczynski, K., Wiktorowicz, G., Fryer, C. L., Holz, D. E., & Kalogera, V. 2012, *ApJ*, 757, 91
- Blaauw, A. 1961, *Bull. Astron. Inst. Netherlands*, 15, 265
- Bodensteiner, J., Shenar, T., Mahy, L., et al. 2020, *A&A*, 641, A43
- Casares, J. 2007, in *IAU Symposium*, Vol. 238, *Black Holes from Stars to Galaxies – Across the Range of Masses*, ed. V. Karas & G. Matt, 3–12
- Casares, J. & Jonker, P. G. 2014, *Space Sci. Rev.*, 183, 223
- de Jager, C., Nieuwenhuijzen, H., & van der Hucht, K. A. 1988, *A&AS*, 72, 259
- Ekström, S., Georgy, C., Eggenberger, P., et al. 2012, *A&A*, 537, A146
- El-Badry, K. & Quataert, E. 2021, *A stripped-companion origin for Be stars: clues from the putative black holes HR 6819 and LB-1*
- Fragos, T., Andrews, J. J., Ramirez-Ruiz, E., et al. 2019, *The Astrophysical Journal*, 883, L45
- Fregeau, J. M., Cheung, P., Portegies Zwart, S. F., & Rasio, F. A. 2004, *MNRAS*, 352, 1
- Fryer, C. L., Belczynski, K., Wiktorowicz, G., et al. 2012, *ApJ*, 749, 91
- Giersz, M. 1998, *MNRAS*, 298, 1239
- Giersz, M., Leigh, N., Marks, M., Hypki, A., & Askar, A. 2014, *ArXiv e-prints* [arXiv:1411.7603]
- Hawking, S. W. 1974, *Nature*, 248, 30
- Heber, U. 2009, *ARA&A*, 47, 211
- Hohle, M. M., Neuhäuser, R., & Schutz, B. F. 2010, *Astronomische Nachrichten*, 331, 349
- Hong, J., Askar, A., Giersz, M., Hypki, A., & Yoon, S.-J. 2020, *MNRAS*, 498, 4287
- Hurley, J. R., Pols, O. R., & Tout, C. A. 2000, *MNRAS*, 315, 543
- Hurley, J. R., Tout, C. A., & Pols, O. R. 2002, *MNRAS*, 329, 897
- Hypki, A. & Giersz, M. 2013, *MNRAS*, 429, 1221
- Mazeh, T. & Faigler, S. 2020, *Does the HR 6819 triple system contain a dormant black hole? Not necessarily*
- Meiron, Y., Webb, J. J., Hong, J., et al. 2021, *MNRAS*, 503, 3000
- Nugis, T. & Lamers, H. J. G. L. M. 2000, *A&A*, 360, 227
- Olejak, A., Belczynski, K., Bulik, T., & Sobolewska, M. 2020a, *A&A*, 638, A94
- Olejak, A., Fishbach, M., Belczynski, K., et al. 2020b, *arXiv e-prints*, arXiv:2004.11866
- Paxton, B., Bildsten, L., Dotter, A., et al. 2011, *ApJS*, 192, 3
- Paxton, B., Cantiello, M., Arras, P., et al. 2013, *ApJS*, 208, 4
- Paxton, B., Marchant, P., Schwab, J., et al. 2015, *ApJS*, 220, 15
- Paxton, B., Schwab, J., Bauer, E. B., et al. 2018, *ApJS*, 234, 34
- Paxton, B., Smolec, R., Schwab, J., et al. 2019, *ApJS*, 243, 10
- Piotto, G., Milone, A. P., Bedin, L. R., et al. 2015, *AJ*, 149, 91
- Rivinius, T., Baade, D., Hadrava, P., Heida, M., & Klement, R. 2020, *A&A*, 637, L3
- Santoliquido, F., Mapelli, M., Bouffanais, Y., et al. 2020, *The Astrophysical Journal*, 898, 152
- Tsuna, D., Kawanaka, N., & Totani, T. 2018, *MNRAS*, 477, 791
- Vink, J. S., de Koter, A., & Lamers, H. J. G. L. M. 2001, *A&A*, 369, 574
- Wang, L., Spurzem, R., Aarseth, S., et al. 2016, *MNRAS*, 458, 1450
- Wyrzykowski, Ł., Kostrzewa-Rutkowska, Z., Skowron, J., et al. 2016, *MNRAS*, 458, 3012

Appendix A Model comparison with MESA

To have a comparison for the pre-CE phase we also simulated the evolution of the BH progenitor in the binary system with MESA (Paxton et al. 2011, 2013, 2015, 2018, 2019). The code version used for this study is the 12778. Figure 7 represents the pre-CE evolutionary track for the primary star in the isolated binary evolution scenario described in section 3.1, according to both MESA and StarTrack.

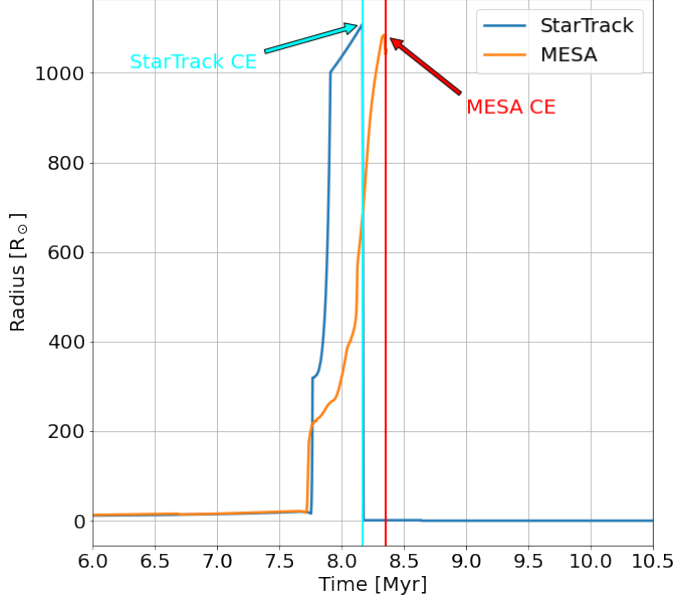


Fig. 7: Comparison between the radius evolution of the pre-CE BH progenitor computed by StarTrack (blue line) and the one retrieved from MESA binary simulations (orange line). The vertical line represents the time at which the mass transfer is supposed to start according to MESA, while the vertical cyan one represents the same for StarTrack simulations. The scenario that has been taken into account consists of a binary with the initial mass for the BH progenitor of $24 M_{\odot}$ and $7 M_{\odot}$ for its stellar companion, with a metallicity of 0.0105 and an initial orbital separation of $2540 R_{\odot}$. According to StarTrack the mass transfer starts at ~ 8.2 Myr with a BH progenitor radius of $1108.9 R_{\odot}$, while similarly the same event start according to MESA at ~ 8.3 Myr and $1084.7 R_{\odot}$. For further description of this evolutionary scenario see section 3.1.

The stellar winds prescription used in StarTrack adopts the winds mass loss ratio for massive stars from Vink et al. (2001) and LBV winds (Belczynski et al. 2010) in the following way:

$$\dot{M}_{\text{lbv}} = f_{\text{lbv}} 10^{-4} [M_{\odot} \text{ yr}^{-1}] \quad (8)$$

with $f_{\text{lbv}} = 1.5$. For MESA we instead used the Dutch wind prescription for massive stars, which means that depending on the effective temperature T_{eff} and the surface hydrogen abundance H_{sur} (in terms of the fraction of hydrogen on the stellar surface) different models are used. As described in Table 5, if $T_{\text{eff}} < 10^4$ K the de Jager et al. (1988) model are used regardless of the hydrogen surface abundance. When $T_{\text{eff}} > 10^4$ K MESA either adopts the Nugis & Lamers (2000) model if $H_{\text{sur}} < 0.4$, or the one from Vink et al. (2001) if the H abundance is instead higher than 0.4.

Table 5: Dutch Stellar Winds prescription in MESA. The choice of the model is based on T_{eff} and, in case of hot stars, also on the hydrogen surface abundance.

	$T_{\text{eff}} < 10^4 \text{ K}$	$T_{\text{eff}} \geq 10^4 \text{ K}$
–	de Jager et al. (1988)	–
$H_{\text{sur}} < 0.4$	–	Nugis & Lamers (2000)
$H_{\text{sur}} \geq 0.4$	–	Vink et al. (2001)

The De Jager winds (de Jager et al. 1988) are defined by the following equation:

$$\log(\dot{M}) = 1.769 \log\left(\frac{L}{L_{\odot}}\right) - 1.676 \log(T_{\text{eff}}) - 8.158 \quad (9)$$

where L is the star luminosity, L_{\odot} is the Sun luminosity, and \dot{M} is in $M_{\odot} \text{ yr}^{-1}$. The wind mass loss for Wolf-Rayet stars is instead described in Nugis & Lamers (2000):

$$\dot{M} = 10^{-11} \left(\frac{L}{L_{\odot}}\right)^{1.29} Y^{1.7} \sqrt{Z} [M_{\odot} \text{ yr}^{-1}] \quad (10)$$

where Z is the metallicity and Y is the He surface abundance. Additionally, mass loss rates in MESA can be adjusted by changing a scaling factor f_{wind} , which for this comparison was kept to 1 (i.e. no adjustment).

Unfortunately a further comparison for the post-CE phase wasn't possible, since in the adopted version of MESA (v.12778) a routine to simulate a whole CE phase has not been implemented yet. Relatively soon after the beginning of the unstable mass transfer the required time step precision to follow the rapid evolution of the BH progenitor becomes unattainable for MESA simulations.

With MESA the mass transfer starts at ~ 8.3 Myr with a radius of $1084.7 R_{\odot}$, while StarTrack reaches the same point at ~ 8.2 Myr and $1108.9 R_{\odot}$. Both radii and stellar ages at the beginning of the mass transfer have a percentage difference of roughly 2% between the two codes. This result shows a satisfactory agreement between the twos, with MESA the mass transfer starts at ~ 8.3 Myr with a radius of $1084.7 R_{\odot}$, while StarTrack reaches the same point at ~ 8.2 Myr and $1108.9 R_{\odot}$. Both radii and stellar ages at the beginning of the mass transfer have a percentage difference of roughly 2% between the two codes. This result shows a satisfactory agreement between the two models for the pre-CE phase.